Numerical Study of Contaminant Transport in Fractured Porous Rock with Distance Dependent Dispersivity

Pramod Kumar Sharma[*1], Sourabh Kakani[2], Sanjay Kumar Shukla[3]

[1,2]Department of Civil Engineering, Indian Institute of Technology, Roorkee, India

[3]Discipline of Civil and Environmental Engineering, School of Engineering, Edith Cowan University, Perth, Australia

*drpksharma07@gmail.com

***Abstract*-This paper presents solute concentration profiles with constant, linear and exponential distance-dependent dispersion models for solute transport through fractured porous rock matrices. A numerical analysis has been developed for solution of the equations governing the dispersion model using the hybrid finite volume method. The results of the numerical analysis have been used to investigate the effect of the matrix diffusion coefficient, fracture velocity, and matrix and fracture retardation factors on concentration profiles. It is found that in the presence of higher matrix diffusion coefficients, the behaviour of concentration profiles is different for constant and distance-dependent dispersion models. However, the behaviour of concentration profiles is observed to be nonlinear during the small transport time period, and the matrix diffusion is found to control the spreading of solute in the fracture in the presence of constant and distance-dependent dispersion models.**

Keywords- Fractured Rocks; Numerical Solution; Distance-dependent Dispersion; Concentration Profiles

I. INTRODUCTION

Fractures within a rock mass are generally preferential pathways along which dissolved reactive and non-reactive contaminants may move rapidly, as the permeability of a fractured rock mass is greater than the permeability of a porous rock [1]. Therefore, it is of practical importance to understand the behaviour of reactive solute transport through the fractured porous media. The dispersion in the fractured porous media is governed by the spatial variability of the groundwater velocity, which is caused by the heterogeneity in hydraulic properties of the media [2]. In the case of solute transport, due to unsteady groundwater flow in a heterogeneous medium, the dispersion coefficient varies with space and is considered to be a function of the distance. The value of dispersivity increases with the travel distance, which is interpreted as a scale effect stemming from flow channelling in the fracture plane [3]. As the geometry of natural fractures in situ cannot be defined and calculations are complicated, a macroscopic approach to the scale effect of channelling therefore appears more realistic. Hence, the dispersion in the fracture can be considered as a function of migration distance.

For the heterogeneous porous media, there are a number of approaches that consider the dispersion coefficient to be either distance-[4-7] or time-dependent [8-10]. A stochastic approach has been used to represent the physical heterogeneity [2], and also several models such as the linear, power law, asymptotic and exponential dispersion models to represent the heterogeneity, of the porous media [4]. The power law model has been used to fit dispersivity values as a function of migration distance [11]. Most of the reference tracer tests have been performed over distances between one to one thousand meters considering both porous and fractured media. An analytical solution has been obtained for linearly increasing dispersion, linear equilibrium sorption and first order degradation for reactive transport through porous media [6]. Also, analytical solutions have been derived for a porous medium with a linear and exponentially increasing dispersion coefficient [12-13]. A semi-analytical solution has been developed for the mobile-immobile model with distance-dependent dispersion [7]. It was found that the distance-dependent dispersion model describes the solute transport more effectively than the constant dispersion model. A hybrid finite volume method was used to solve the non-equilibrium transport model for solute in the fracture and study the behavior of concentration profiles with different transport parameters [14].

In the case of fractured porous rocks, there are limited studies that use the distance-dependent dispersivity model. In this paper, the behaviour of both temporal and spatial solute concentration profiles have been presented for the solute transport in the fractured porous formation for constant, linear and exponential distance-dependent dispersion models. The governing equations for the distance-dependent dispersion models have been solved using a hybrid finite volume method. The developed numerical model has been used to study the effects of various transport parameters on the solute concentration profiles using constant, linear and exponential distance-dependent dispersion models.

II. CONCEPTUAL MODEL OF REACTIVE TRANSPORT IN FRACTURED POROUS ROCKS

Rock masses contain discontinuities of different types and sizes, such as faults, joints, fracture zones and bedding planes [15]. The rock matrix contains the fine-grained mass of rock material in which larger grains and crystals are embedded. The conceptual model for the solute transport through a fractured porous rock is shown in Fig. 1. The fractured porous rock

DOI: 10.5963/JWRHE0502001

consists of parallel plate-like fractures of width $2b$. The fluid moves through the fracture in the X - direction with velocity V_f. The reactive tracers in the fluid phase within the porous rock mix with those in the fluid phase in the fractures by diffusion. It is assumed that there was no fluid flow in the porous matrix. In the fractured porous rock system, the solute transport in the fracture must be treated separately from the transport in the porous rock slabs. The transport in the fracture occurred through fluid advection in the X - direction, and the transport in the rock slabs takes place as a diffusion through the pore fluid in the Y - direction.

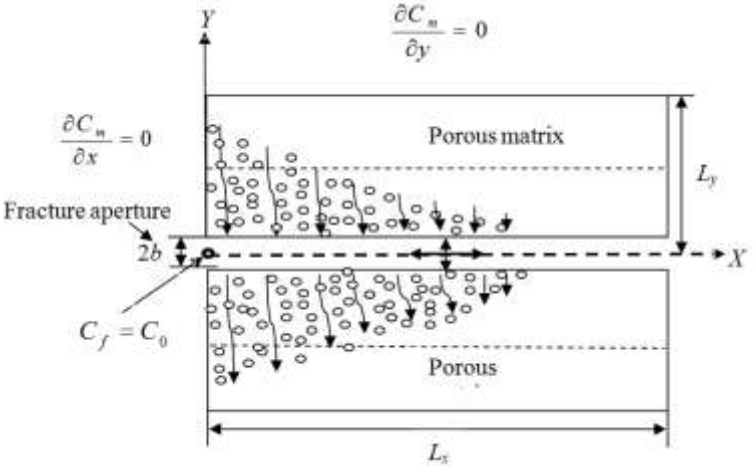

Fig. 1 A conceptual model for the solute transport through the fractured porous matrix

III. GOVERNING EQUATIONS FOR SOLUTE TRANSPORT

The transport processes in the fracture porous rock system are described by two coupled equations, one for the fracture and the other for the porous rock matrix. The coupling is accounted for by a diffusive mass transfer between the fracture and the adjacent porous matrix. In this study, the following processes are considered: advection and longitudinal dispersion in the fracture, molecular diffusion from the fracture into the rock matrix, and adsorption and decay in the fracture and matrix. The coupling between the fracture and the porous rock is represented by the continuity of fluxes and concentrations along the interface [16]. The matrix diffusion is regarded as a one-dimensional process, which is justified by the assumption that transport along the fracture is much faster than transport within the matrix. Diffusion exchanges along the direction parallel to the fracture plane are then negligible as compared with those perpendicular to the fracture plane. A diffusive transport equation considering the linear equilibrium sorption and the first order degradation for the porous rock matrix can be written as [16]:

$$R_m \frac{\partial C_m}{\partial t} = D_m \frac{\partial^2 C_m}{\partial y^2} + \lambda R_m C_m \tag{1}$$

where $C_m = C_m(x, y, t)$ is the contaminant concentration of solute in solution (M/L^3); D_m is the effective diffusion coefficient (L^2/T); λ is the decay rate constant (T^{-1}); R_m is the matrix retardation factor, defined as: $R_m = 1 + \frac{\rho_m}{\theta} K_m$; ρ_m is the bulk density of the porous rock matrix (M/L^3); K_m is the distribution coefficient (L^3/M), which is a ratio of the mass of solute adsorbed per unit weight of solid and the concentration of solute in solution, and is equal to the slope of the sorption isotherm; and θ_m is the porosity of the rock matrix.

The advective dispersive transport equation, including the linear equilibrium sorption and the first order degradation for fracture, can be written as [16]:

$$\frac{\partial C_f}{\partial t} + \frac{V_f}{R_f}\frac{\partial C_f}{\partial x} = \frac{1}{R_f}\frac{\partial}{\partial x}\left[D_f \frac{\partial C_f}{\partial x}\right] + \left(\frac{\theta_m D_m}{b R_f}\right)\frac{\partial C}{\partial y} - \lambda C_f \tag{2}$$

where $C_f = C_f(x, t)$ is the contaminant concentration of the solute in the solution (M/L^3); b is the half fracture aperture (L); V_f is the fracture groundwater velocity (L/T); D_f is the dispersion coefficient (L^2/T); and R_f is the retardation coefficient

DOI: 10.5963/JWRHE0502001

in the fracture, defined as $R_f = 1 + \frac{K_f}{b}$, where K_f is the fracture distribution coefficient (L), defined as the ratio of mass of solute adsorbed per unit surface area of fracture and the concentration of solute in the solution [17]. As discussed earlier, both the distance dispersivity and the exponential distance-dependent dispersivity were used in the literature. As per [12], the distance- dependent dispersion coefficient is given by:

$$D_f(x) = \alpha_f(x) V_f + D_0 = K x V_f + D_0 \tag{3a}$$

where $\alpha_f(x)$ is the distance-dependent dispersivity (L), K is the slope of the dispersivity-distance relationship (L^0) (i.e., the dispersivity / distance ratio), and x is the distance from the source (L).

In Equation (3a), the dispersivity increases linearly with the travel distance; therefore, it is also called the linear distance-dependent dispersivity function [12]. The exponential distance-dependent dispersion coefficient can be represented as [13]:

$$D_f(x) = \alpha(x) V_f + D_0 = a_1\left(1 - e^{-b_1 x}\right) V_f + D_0 \tag{3b}$$

where $\alpha_f(x)$ is the exponential distance-dependent dispersivity (L) and D_0 is the molecular diffusion coefficient (L^2/T).The following initial and boundary conditions for the fracture and porous rock matrix have been considered in the present study:

$$C_f(x,0) = 0; \quad C_f(0,t) = C_0; \quad \left.\frac{\partial C_f}{\partial x}\right|_{(\infty,t)} = 0 \tag{4a}$$

$$C_m(x,y,0) = 0; \quad C_m(x,b,t) = C_f(x,t); \quad \left.\frac{\partial C_m}{\partial y}\right|_{(x,L_y,t)} = 0 \tag{4b}$$

where C_0 is the initial injected concentration of the solute at the inlet of the fracture (M/L^3).

A. Numerical Formulation

In the present study, the governing transport equations for the porous rock matrix and the fracture were solved using a hybrid finite volume method [18]. The governing equations were solved using the operating splitting approach for advection and dispersion. On applying the operator split approach, Equation (2) can be written as:

$$\frac{\partial C_f}{\partial t} = -\frac{V_f}{R_f}\frac{\partial C_f}{\partial x} \tag{5a}$$

$$\frac{\partial C_f}{\partial t} = \frac{1}{R_f}\frac{\partial}{\partial x}\left[D_f \frac{\partial C_f}{\partial x}\right] \tag{5b}$$

$$\frac{\partial C_f}{\partial t} = \left(\frac{\theta_m D_m}{b R_f}\right)\frac{\partial C_m}{\partial y} - \lambda C_f \tag{5c}$$

Equations (5a), (5b) and (5c) represent the advective, dispersion and reaction terms of Equation (2).

B. Solution of Advection Transport Term

The finite volume method was used to solve the advective transport (Equation 5a) using the monotone upwind schemes for conservation laws (MUSCL) given by [19]. The scheme was globally higher order accurate and non-oscillatory [18]. The implicit finite volume scheme is written as [20]:

$$C_{fa\,j}^{t+1} = C_{f\,j}^{t} - \frac{\Delta t}{\Delta x}\left[\theta\left(\bar{F}_{j+1/2}^{t+1} - \bar{F}_{j-1/2}^{t+1}\right) + (1-\theta)\left(\bar{F}_{j+1/2}^{t} - \bar{F}_{j-1/2}^{t}\right)\right] \tag{6}$$

where $C_{fa\,j}^{t+1}$ is the concentration at j cell at the end of the advective computation step. The parameter θ controls the degree of implicitness of the above equation; $\theta =$ 0, 0.5 and 1.0 will give explicit, second order implicit and first order implicit

DOI: 10.5963/JWRHE0502001

schemes, respectively. Here, $\bar{F}_{j+1/2}^{t}$ and $\bar{F}_{j+1/2}^{t+1}$ denote the advective flux at known and unknown time levels, i.e., at t and $t+1$, respectively, and j and $j+1$ are node numbers. Fluxes at the cell interface of j and $j+1$ are evaluated as:

$$\bar{F}_{j+1/2}^{t} = \frac{V_{fj}}{R_f} C_{f\,j+1/2}^{L} \text{ When } V_{f_i} > 0 \tag{7a}$$

Otherwise,

$$\bar{F}_{j+1/2}^{t} = \frac{V_{f\,j+1}}{R_f} C_{f\,j+1/2}^{R} \tag{7b}$$

where $C_{f\,j+1/2}^{R} = C_{f\,j+1} - \frac{1}{2}\delta C_{f\,j+1}$ and $C_{f\,j+1/2}^{L} = C_{f\,j} + \frac{1}{2}\delta C_{f\,j}$, $\delta C_{f\,j}$ is the gradient of the concentration distribution in the cell j, and L and R represent the left and right faces of the cell interface, respectively. The value of $\delta C_{f\,j}$ is computed using the minmod limiter.

$$\delta C_{f\,j} = ave\left(\Delta_1 C_{f\,j}, \Delta_2 C_{f\,j}\right) \tag{7c}$$

$$\begin{aligned} ave\left(\Delta_1 C_{f\,j}, \Delta_2 C_{f\,j}\right) &= sign(\Delta_1 C_{f\,j}) \min\left(\Delta_1 C_{f\,j}, \Delta_2 C_{f\,j}\right) \quad \text{if } \left(\Delta_1 C_{f\,j} \Delta_2 C_{f\,j} > 0\right) \\ &= 0 \qquad \text{Otherwise} \end{aligned} \tag{7d}$$

where $\Delta_1 C_{f\,j} = C_j - C_{j-1}$ and $\Delta_1 C_{fi} = C_{j+1} - C_j$.

For the non-oscillatory property, the Courant number restriction for an implicit scheme is given by [20]:

$$\theta = \max\left(0.5, 1 - \frac{0.5}{Cr}\right) \tag{8}$$

where C_r is the Courant number, which is given by $C_r = \frac{V_f . \Delta t}{\Delta x}$, and Δt and Δx are time step and grid size, respectively.

C. Solution of Dispersive and Reactive Transport Term

The dispersive transport (Equation 5b) was performed on the concentrations, resulting from the advective transport in each time step. A conventional, fully implicit, finite-difference scheme was used to obtain the final concentrations at the end of each time step. The formulation is given as:

$$\frac{C_{f_i}^{l+1} - C_{f_i}^{l}}{\Delta t} = \frac{D_f}{R_f (\Delta x)^2}\left[D_{f_{i+1}}^{l+1}\left(C_{f_{i+1}}^{l+1} - C_{f_i}^{l+1}\right) - D_{f_i}^{l+1}\left(C_{f_i}^{l+1} - C_{f_{i-1}}^{l+1}\right)\right] \tag{9}$$

The reaction term given by Equation (5c) is solved by the fourth order Range-Kutta method. The coupling of the transport with the reactive part is achieved during a time step by using a sequential process in which Equations (5a) and (5b) are solved in the first step, and then the reactive part is solved in the second step. The diffusive transport equation of the porous matrix, that is, Equation (1), was solved by the finite difference method.

D. Verification of the Numerical Model

For verification of the developed numerical model, the spatial relative concentration profiles (for a constant concentration boundary condition) were compared with the analytical solution of the transport equation with a distance-dependent dispersion coefficient [7].

Fig. 2 shows the spatial concentration profile for a linear distance-dependent dispersion model with constant boundary conditions. Also, the developed numerical model for the constant dispersion model for reactive solute transport in a fractured porous rock was verified with the analytical solutions given by [21], as shown in Fig. 2. An excellent match was obtained between the numerical and the analytical results. Thus, the developed numerical model has been found to be appropriate for the

DOI: 10.5963/JWRHE0502001

detailed analysis of the concentration profiles for several cases.

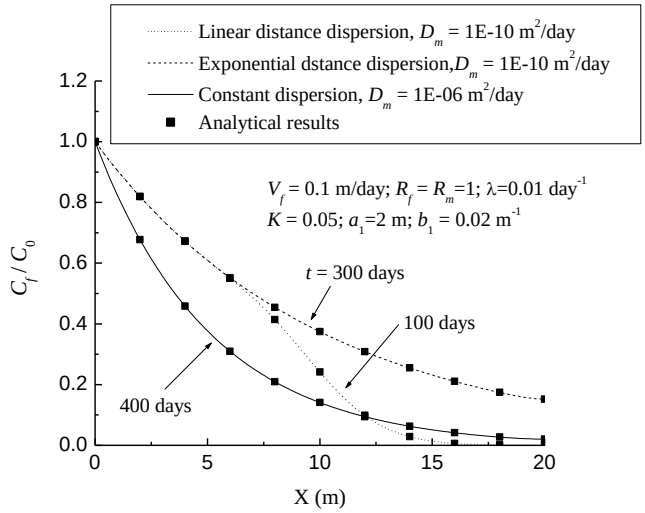

Fig. 2 Comparison of spatial concentration profiles with numerical and analytical results for solute in the fracture for constant, linear and exponential distance-dependent dispersion models

IV. RESULTS AND DISCUSSION

The numerical model was used to predict both spatial and temporal concentration profiles for solute in the fracture with constant, linear and exponential distance-dependent dispersion models. The value of fracture spacing $L_y = 0.01\text{m}$, length of the fracture $L_x = 20$ m, constant fracture dispersivity α_f =1 m, linear distance dependent coefficient K=0.05 and exponential distance dependent coefficients a_1=2 m and b_1=0.02 m^{-1} were taken during the prediction of the results of the concentration profiles. The values of the other transport parameters were mentioned in the corresponding figures. The effects of transport parameters on concentration profiles are discussed below.

A. Effect of Matrix Diffusion Coefficient

The concentration profiles were compared in the presence of lower (D_m =1E-10 m^2/day) and higher (D_m =1E-06 m^2/day) values of effective matrix diffusion coefficients. Spatial solute concentration profiles were computed at 10, 20, 40 and 60 days along the fracture, as shown in Figs. 3a and 3b.

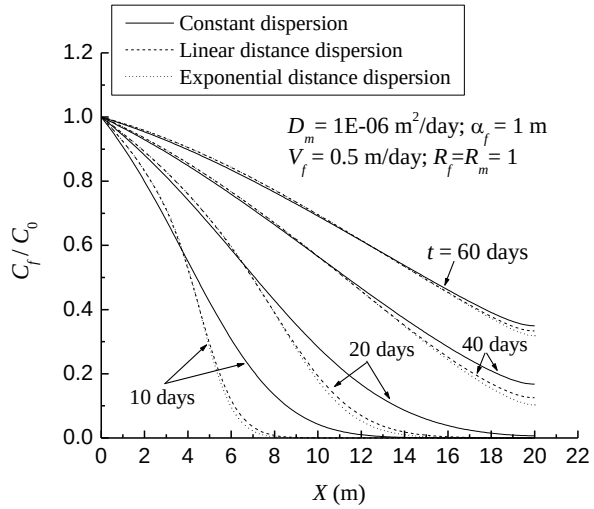

Fig. 3a Spatial concentration profiles for the solute in the fracture predicted at different transport times with higher value of effective diffusion coefficient (D_m=1.E-06 m^2/day)

DOI: 10.5963/JWRHE0502001

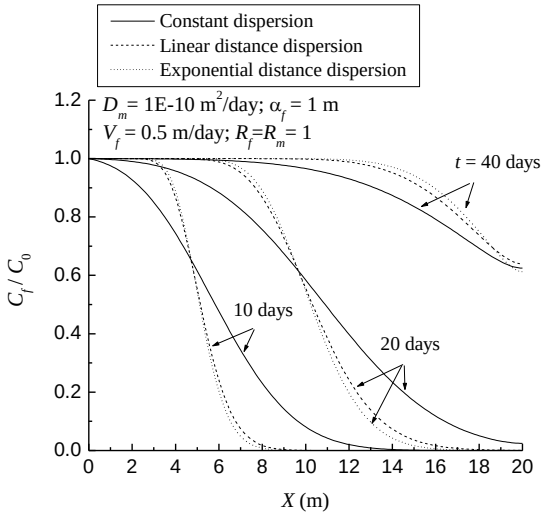

Fig. 3b Spatial concentration profiles for the solute in the fracture predicted at different transport times with lower value of effective diffusion coefficient (D_m=1.E-10 m^2/day)

Figs. 4a and 4b represent the temporal concentration profiles at 5, 10 and 20 m down gradient distance in the flow direction. The behavior of the spatial and temporal concentration profiles remains the same in cases of linear and exponential dispersion models. However, a large variation occurs in between constant and distance-dependent dispersion models due to an increase in the value of dispersivity with travel distance. The variation in the magnitude of the solute concentration is different during small time and higher transport time. In presence of a higher value of the matrix diffusion coefficient, the difference in the magnitude of solute concentration is observed for constant and distance-dependent dispersion models during a short transport time. However, during a long transport time period, the magnitude of the solute concentration remains the same for both cases of constant and distance-dependent dispersion models. This means that the presence of matrix diffusion also affects the behavior of the solution concentration in the fracture.

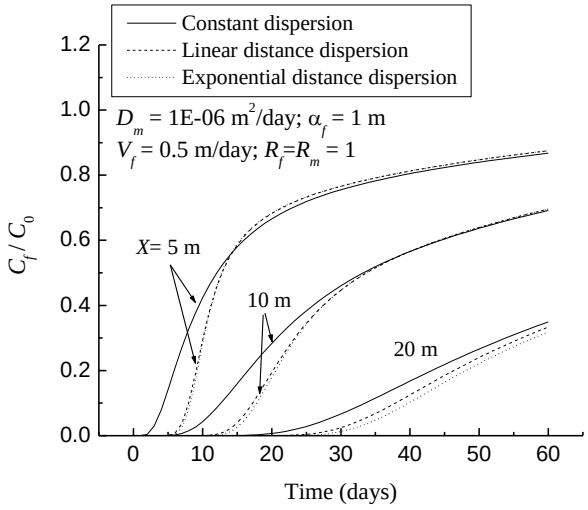

Fig. 4a Temporal concentration profiles for the solute in the fracture predicted at travel distance with higher value of effective diffusion coefficient (D_m=1.E-06 m^2/day)

DOI: 10.5963/JWRHE0502001

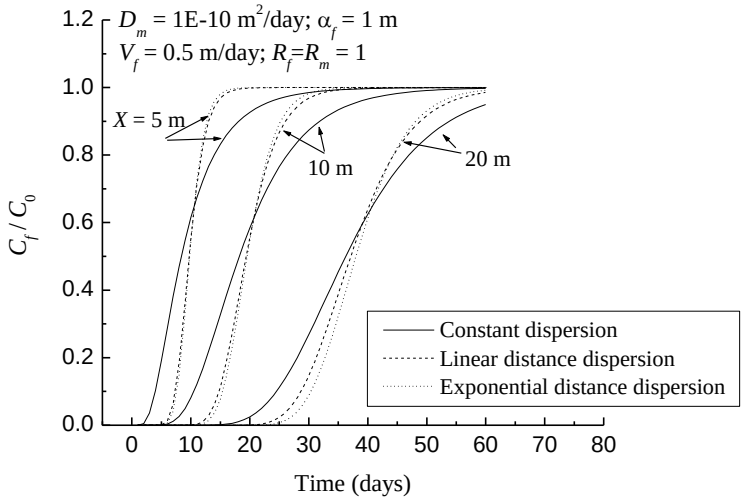

Fig. 4b Temporal concentration profiles for the solute in the fracture predicted at different travel distances with lower value of effective diffusion coefficient (D_m=1.E-10 m^2/day)

B. Effect of Fracture Pore Water Velocity

The temporal and spatial concentration profiles for the solute in the fracture with different fracture velocities for constant, linear and exponential distance-dependent dispersion coefficients are shown in Figs. 5a and 5b, respectively. As expected, a higher value of fracture pore water velocity (V_f = 0.6 m/day) increased the magnitude of the solute concentration in the fracture and the magnitude remained the same for the case of constant, linear and exponential dispersion models. However, in cases of small value of fracture velocity, the magnitude of the solute concentration was reduced and the variation was observed for the case of constant and distance-dependent dispersion models.

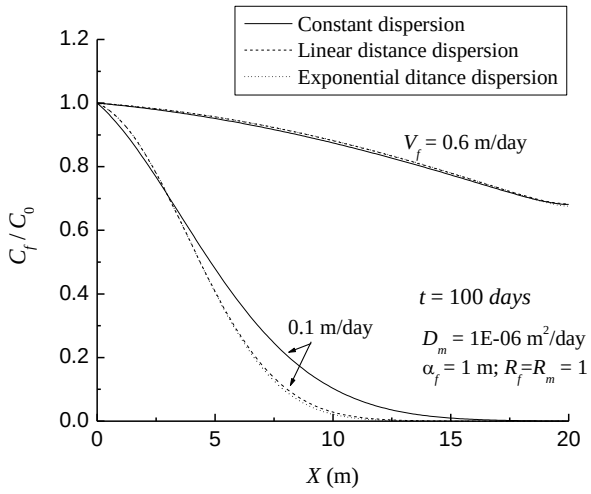

Fig. 5a Spatial concentration profiles for the solute in the fracture with two different values of fracture groundwater velocity

DOI: 10.5963/JWRHE0502001

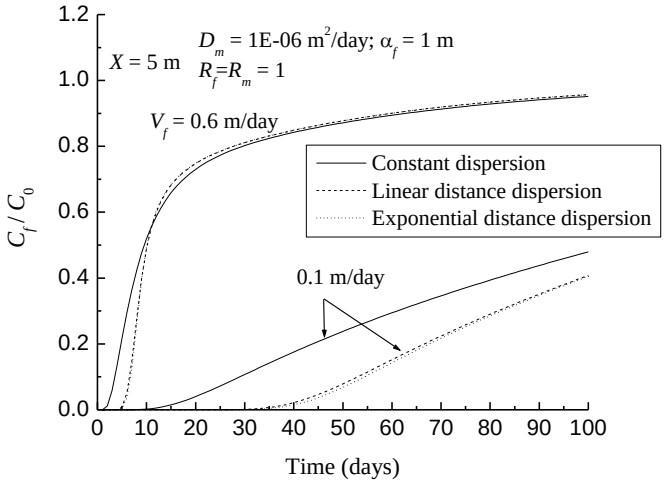

Fig. 5b Temporal concentration profiles for the solute in the fracture with two different values of fracture groundwater velocity

C. Effect of of Fracture and Matrix Retardation Factor

Figs. 6a and 6b show the spatial and temporal concentration profiles with different values of fracture retardation factor. It is observed that a large value of the fracture retardation factor (R_f =10) reduced the magnitude of the solute concentration in the fracture, and variation in the magnitude of the solute concentration was observed for constant and distance-dependent dispersion models. The magnitude of the solute concentration remained the same for a small value of fracture retardation factor (R_f =1) for constant, linear and exponential distance-dependent dispersion models. At a small travel distance, the magnitude of the solute concentration was higher in the distance-dependent dispersion model than it was in the constant dispersion model. However, at a large travel distance, the magnitude of the solute concentration was smaller in the distance dependent dispersion than the constant dispersion model. It is also seen that the behavior of the spatial concentration profiles was nonlinear. Similarly, the behavior of the temporal concentration profiles predicted at 5 m down gradient distance was observed for the constant and distance-dependent dispersion models.

However, in the presence of a higher retardation factor, the behavior of the concentration profiles was different, and early arrival of solute concentration was observed for the case of the constant dispersion model as compared to the distance-dependent dispersion model. The behavior of the spatial and temporal concentration profiles (Figs. 7a and 7b) remained the same in the presence of a matrix retardation factor for constant, linear and exponential distance-dependent dispersion models. It is noticed that a higher value of matrix retardation factor led to a lower magnitude of solute concentration in the fracture.

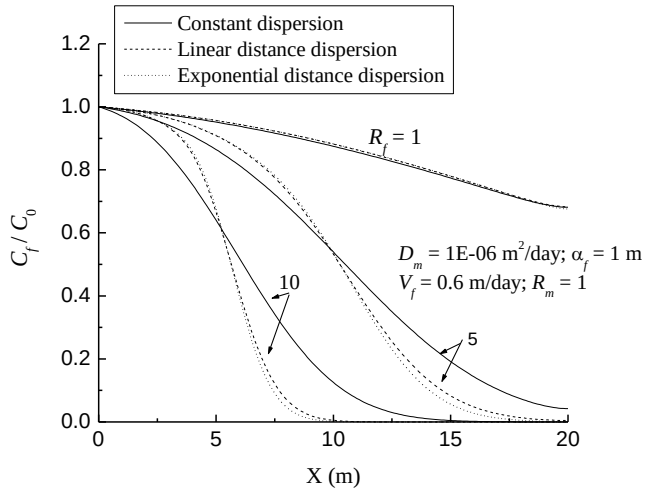

Fig. 6a Spatial concentration profiles for the solute in the fracture with different values of fracture retardation factor

DOI: 10.5963/JWRHE0502001

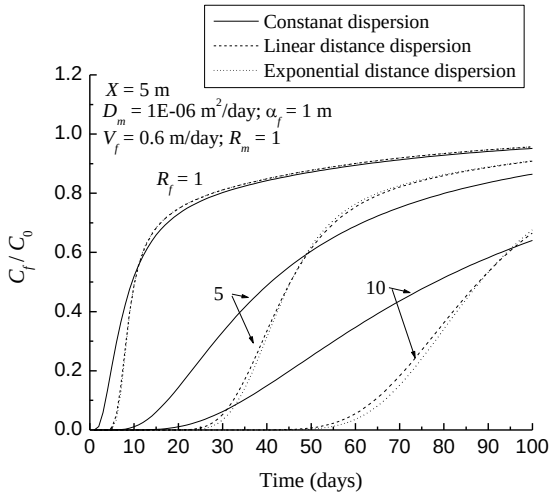

Fig. 6b Temporal concentration profiles for the solute in the fracture with different values of fracture retardation factor

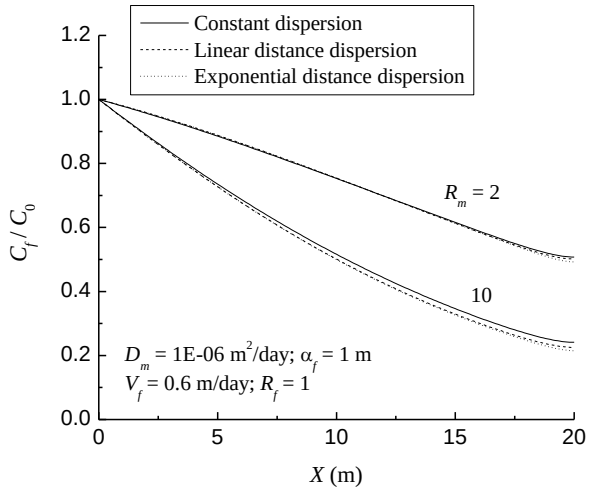

Fig. 7a Spatial concentration profiles for the solute in the fracture with two different values of matrix retardation factor

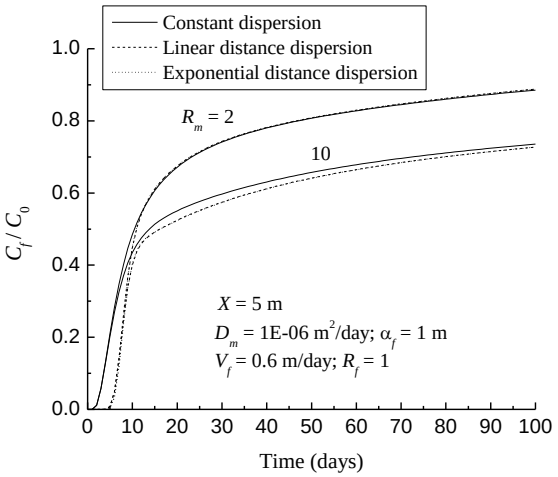

Fig. 7b Temporal concentration profiles for the solute in the fracture with different values of matrix retardation factor

DOI: 10.5963/JWRHE0502001

D. Effect of Decay Rate Coefficients

Figs. 8a and 8b represent the spatial and temporal concentration profiles with different values of decay rate coefficient for constant, linear and exponential distance-dependent dispersion models.

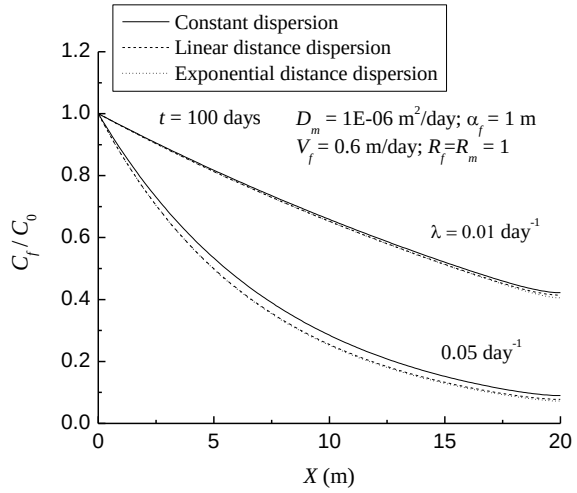

Fig. 8a Spatial concentration profiles for the solute in the fracture with two values of first order decay rate coefficients

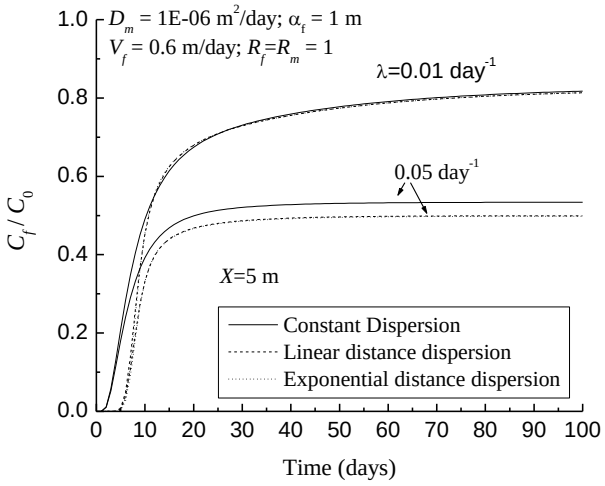

Fig. 8b Temporalconcentration profiles for the solute in the fracture with different values of first order decay rate coefficients

It is observed that a higher value of decay rate coefficient reduced the magnitude of the solute concentration in the fracture. For a higher value of decay rate coefficient, the magnitude of the solute concentration was smaller in the case of distance-dependent dispersion as compared to the constant dispersion model. However, in the presence of a smaller decay rate coefficient, the magnitude of the solute concentration remained the same for the constant and distance-dependent dispersion models. In the presence of a higher value of decay rate coefficient, a small variation in magnitude of the solute concentration was observed for the constant and distance-dependent dispersion models.

E. Effect of Fracture Spacing

The spatial and temporal concentration profiles for different fracture spacings in the presence of constant, linear and exponential distance-dependent dispersion models are shown in Figs. 9a and 9b. It can be seen that the magnitude of the relative solute concentration reduced linearly in the flow direction in the presence of small value of fracture spacing. The magnitude of the spatial relative solute concentration remained the same for the case of the constant, linear and exponential distance-dependent dispersion models. However, with a short transport time period, the magnitude of the solute concentration was higher in the case of the distance-dependent dispersion as compared to the constant dispersion model. This is due to the fact that the value of the distance-dependent dispersion coefficient changes in the flow direction.

DOI: 10.5963/JWRHE0502001

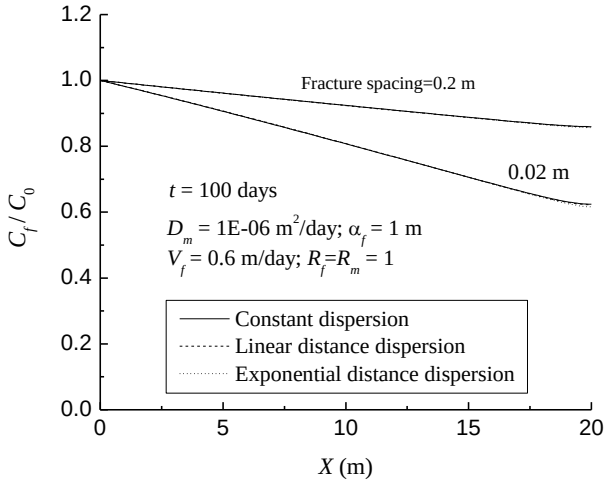

Fig. 9a Spatial concentration profiles for the solute in the fracture with two different values of fracture spacing

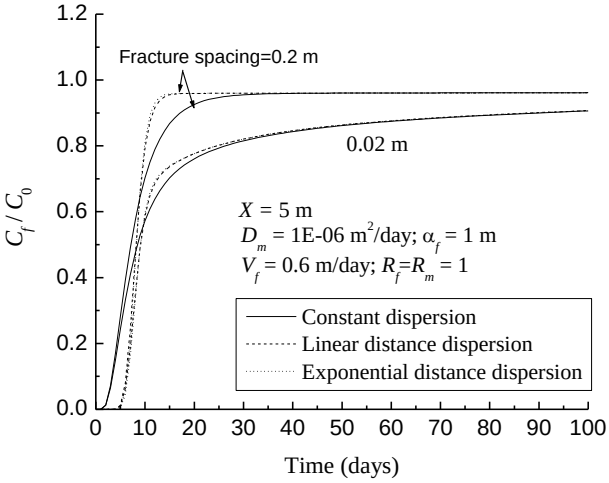

Fig. 9b Temporalconcentration profiles for the solute in the fracture with two different values of fracture spacing

In the presence of smaller values of the matrix diffusion coefficient, the magnitude of the solute concentration was found to be lower in case of distance-dependent dispersion model during transport times of 10 days and 20 days along a large travel distance. This may be due to fact that distance-dependent dispersion and dispersion contribute to the overall dispersion in the fracture. However, in the case of higher values of the matrix diffusion coefficient, the magnitude of the solute concentration remained the same at a transport time of 60 days. This means that the matrix diffusion controls the spread of the solute in the fracture with distance-dependent dispersion. It can also be seen that the distance-dependent dispersion coefficient did not affect the magnitude of the solute concentration with constant dispersion in the presence of higher values of fracture velocity. An earlier arrival time of the solute was observed in the case of the constant dispersion as compared to the distance-dispersion models, and at a larger transport time, an identical solute concentration was observed.

V. CONCLUSIONS

In this study, a hybrid finite volume method has been used to solve the governing transport equation for the solute in a fracture in the presence of constant dispersion, distance and exponential distance-dependent dispersion models. The effect of transport parameters on concentration profiles has been investigated in the presence of a matrix diffusion coefficient and a distance dispersion model. Based on the results and the discussion, the following general conclusions can be made:

1. Both linear and exponential distance-dependent dispersion models behave similarly, and the difference between the concentration profiles computed by both of these models is found to be very small for most concentration profiles. However, it is observed that the linear and exponential distance-dependent dispersion models behave significantly different from a constant dispersion model in the presence of higher values of the matrix diffusion coefficient.

DOI: 10.5963/JWRHE0502001

2. Higher values of matrix diffusion, retardation factor, and decay rate coefficients lead to a decrease in the magnitude of the solute concentration in the fracture. This means that the mass of solute is transferred from the fracture to the porous matrix.
3. The behavior of concentration profiles is non-linear during the small time period of transport. It is also observed that a smaller value of fracture spacing linearly reduces the magnitude of the solute concentration in the fracture.

ACKNOWLEDGMENT

We would like to acknowledge the endeavour fellowship program, Australia and ECU Perth, Australia for supporting the research work during the period of May-November, 2015.

REFERENCES

[1] C.F. Tsang and I. Neretnieks, "Flow channeling in heterogeneous fractured rocks," *Rev. Geophys*., vol. (36), pp. 275-298, 1998.

[2] L. W. Gelhar, "Stochastic subsurface hydrology," *Prentice-Hall, Englewood Cliffs, N.J*, 1993, pp. 96-110.

[3] J. Bodin, F. Delay, and G. De Marsily, "Solute transport in a single fracture with negligible matrix permeability: 2. mathematical formalism," *Hydrogeology Journal*, vol. 11(4), pp. 434-454, 2003.

[4] J. F. Pickens and G. E. Grisak, "Modeling of scale-dependent dispersion in hydrogeologic systems," *Water Resour Res.*, vol. 17(6), pp. 1701-1711, 1981.

[5] F.J. Moltz, O. Guven, and J.G. Melville, "An examination of scale-dependent dispersion coefficients," *Ground Water*, vol. 21(6), pp. 715-725, 1983.

[6] L. Pang and B. Hunt, "Solutions and verification of scale-dependent dispersion model," *J. Contam. Hydro*., vol. 53, pp. 21-39, 2001.

[7] G. Gao, H. Zhan, S. Feng, B. Fu, Y. Ma, and G. Huang, "A new mobile-immobile model for reactive solute transport with scale-dependent dispersion," *Water Resour. Res*., vol. 46, pp. W08533, doi: 10.1029/2009WR008707, 2010.

[8] R. Srivastava, P.K. Sharma, and M.L. Brusseau, "Spatial moments for reactive transport in heterogeneous porous media," *J. Hydrol. Eng., ASCE*, vol. 7(4), pp. 336-341, 2002.

[9] L. Zhou and H. M Selim, "Scale dependent dispersion in soil: an overview," *Adv., Agron*., vol. 80, pp. 223-263, 2003.

[10] P. K. Sharma and R. Srivastava, "Concentration profiles and spatial moments for reactive transport through porous media," *J of Hazardous, Toxic, and Radioactive Waste, ASCE*, vol. 16(2), pp. 125-133, 2012.

[11] S.P. Neuman, "Universal scaling of hydraulic conductivities and dispersivities in geologic media," *Water Resour. Res*., vol. 26(8), pp. 1749-1758, 1990.

[12] S.R. Yates, "An analytical solution for one-dimensional transport in heterogeneous porous media," *Water Resour. Res*., vol. 26(10), pp. 2331-2338, 1990.

[13] S.R. Yates, "An analytical solution for one-dimensional transport in porous media with an exponential dispersion function," *Water Resour. Res*., vol. 28(8), pp. 2149-2154, 1992

[14] P.K. Sharma, N. Joshi, R. Srivastava, and C.S.P. Ojha, "Reactive Transport in Fractured Permeable Porous Media," *J. Hydrol. Eng*., 10.1061/(ASCE)HE.1943-5584.0001096, 04014078, vol. 20(7), 2014.

[15] L. Jing, O. Stephansson, "Fundamentals of Discrete Element Methods for Rock Engineering: Theory and Applications," (Vol. 85). pp. 147-150, Elsevier, 2007.

[16] D.H. Tang, E.O. Frind, and E.A. Sudicky, "Contaminant transport in fractured porous media: Analytical solution for a single fracture," *Water Resour. Res.*, vol. 17(3), pp. 555-564, 1981.

[17] R. A. Freeze and J.A. Cherry, "Groundwater," *Prentice-Hall, Englewood Cliffs, N.J*., pp. 408-412, 1979.

[18] M. Putti, W. Yeh, and W. A. Mulder, "A triangular finite volume approach with high resolution upwind terms for the solution of ground water transport equations," *Water Resour. Res*., vol. 26(12), pp. 2865-2880, 1990.

[19] B. Van Leer, "Towards the ultimate conservative difference scheme: A new approach to numerical convection," *J. Comput. Phys*., vol. 23, pp. 276-299, 1977.

[20] M.H. Wilcoxson and V. I. Manousiouthakis, "On an implicit eno scheme," *J. Comput. Phys.*, vol. 115, pp. 376-389, 1994.

[21] E. A. Sudicky and E. O. Frind, "Contaminant transport in fractured porous media: Analytical solutions for a system of parallel fractures," *Water Resour. Res*., vol. 18(6), pp. 1634-1642, 1982.

DOI: 10.5963/JWRHE0502001